NUMERICAL STUDIES OF A HYBRID CYCLE FOR POWER PRODUCTION AND COOLING

Nicolas Voeltzel[1], Hai Trieu Phan[1], Nicolas Tauveron[1], Brigitte Gonzalez[1], Quentin Blondel[1], Mathilde Wirtz[1] and François Boudehenn[1]

[1] Univ. Grenoble Alpes, CEA, LITEN, DTBH. F-38000 Grenoble, France

Abstract

This work aims at studying and developing a thermodynamic heat recovery cycle for the combined production of cold energy and low power electricity (5 kW of cold, 1 kW of electricity) using water/ammonia as working fluid. The target temperature range is low enough (80 to 160 °C) to adapt not only industrial heat recovery applications, but also heat networks and non-concentrated solar thermal energy. Thermodynamic modeling of the cycle was carried out and a parallel architecture was proposed, in which the refrigerant vapor at the output of the generator can be used to feed the expander (production of electricity) and/or the condensation-expansion-evaporation part (production of cold). For accurate prediction of the power production, a semi-empirical model of a scroll-type expander was developed based on experimental testing of an organic Rankine cycle (ORC). The numerical data were analyzed in order to identify the key parameters influencing the performance of the present hybrid cycle.

Keywords: Cooling, Power Production, Absorption, Scroll expander, Hybrid cycle

Nomenclature

Quantity	Symbol	Unit
Area	A	mm^2
Exchanged Heat	Q	J
Overall heat transfer coefficient	U	$W\ m^{-2}\ K^{-1}$
Temperature	T	°C
Efficiency	η	
Expander generated power	$\dot{W}$	kW
Mass flow rate	$\dot{m}$	$kg.s^{-1}$
Specific enthalpy	h	$kJ.kg^{-1}$
Friction coefficient	τ_{loss}	N
Split ratio	r_s	

Quantity	Subscript
Expander	$expa$
Experimental	exp
Numerical	U
Expander inlet	in
Expander outlet	Out
Critical	c
Coefficient of Performance	COP
Combined Cooling and power	CCP
Organic Rankine Cycle	ORC
Hydrofluorocarbons	HFC
Built-in Volume Ratio	BVR

1. Introduction

The literature depicts various architectures of combined cooling and power (CCP) production. A first overview of the systems studied was proposed by Ayou *et al.* (2013). Two main families stand out: the cogeneration architectures in series (Xu, Yogi Goswami and S. Bhagwat, 2000; Muye *et al.*, 2016; Khaliq, 2017) and those in parallel (Wang *et al.*, 2009; Mendoza, Ayou, *et al.*, 2014; Kumar, Saravanan and Coronas, 2017). The architectures in series are generally more efficient for simultaneous co-generation of cold and electricity while the architectures in parallel enable more flexibility in term of production. Paralle architecture are also easier to implement because only two levels of pressure are present. Independently of the architectures, the cold can be produced using the principle of the absorption chillers (Mendoza, Ayou, *et al.*, 2014; Muye *et al.*, 2016; Kumar, Saravanan and Coronas, 2017) or that of the ejectors (Khaliq, 2017). The combination of both technologies was also considered in several studies (Alexis, 2007; Wang *et al.*, 2009). Electricity is produced by the expansion of the working fluid in an expander (volumetric type or turbine) coupled to a generator. The development of expanders notably benefits from the recent study of organic fluid Rankine cycles (ORC) (Tauveron, Colasson and

doi:10.18086/swc.2019.55.11 Available at http://proceedings.ises.org

Gruss, 2014).

As cogeneration systems are quite complex cycles, only a few experimental investigations have been conducted so far and they usually simulate hard-provisioning components with simplified equivalents (Kumar, Saravanan and Coronas, 2017). In return, the numerical approach is widely used to explore the performance of innovative architectures. Concerning cooling production, the physical models that describe the various components of thermodynamic cycles have already been well investigated and have led to numerous numerical studies of both absorption and compression machines (Herold, Radermacher and Klein, 2016). Concerning power production, expander models need further investigation due to complex phenomena and a wide range of existing technologies.

Lemort *et al.* (2009) developed a first scroll expander model. This semi-empirical model takes into account the physics related to the transformation of the fluid from the inlet to the outlet of a scroll. In CCP systems coupling an absorption cycle with an expander, the expanded gas in the expander is most often ammonia containing traces of water. Hence, there is a real interest in adapting this model to work with ammonia. Based on experimental data, Mendoza et al. (2014) developed a simplified version of Lemort's model with ammonia as working fluid. The model is later included into a CCP cycle (Mendoza et al., 2014) and the performance of a scroll expander is then calculated for three different working fluids.

As a continuous of the literature work, the present study aims to optimize the performance of CCP cycles. A parallel architecture of the expander integrated into an ammonia-water absorption chiller has been studied. Numerical models of the cycle were developed with a detailed model of a scroll-type expander. Tests were also conducted on the ORC and absorption-chiller machines available in our laboratory, giving experimental data for calibration of the model parameters and boundaries. The simulation results were then analyzed, giving us information about the key factors affecting the cycle performance.

2. Cycle description

The CCP cycle considered in the present study is shown in Figure 1. It consists of a water-ammonia absorption cycle in parallel with an ORC cycle, the one using part of the desorbed ammonia as a working fluid and a scroll expander for power production.

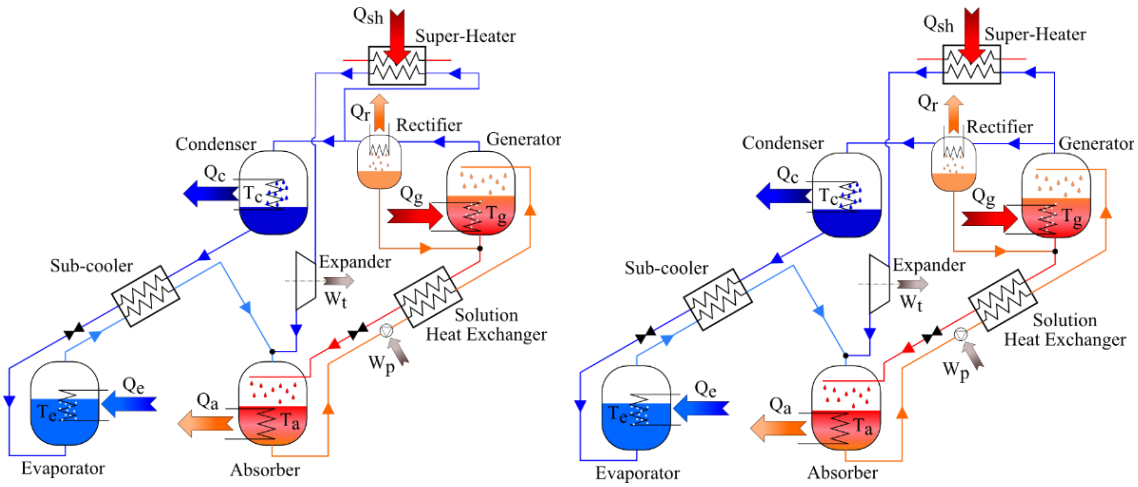

a) Configuration A b) Configuration B

Figure 1. Scheme of the CCP cycle with two different configurations.

On the solution circuit loop, a first line of ammonia-rich solution flows from the absorber to the generator through pressurization by a pump. A second line with an expansion valve brings the poor solution back to the absorber. An economizer preheats the rich solution with the poor solution coming out of the generator.

Upstream of the production lines, a rectifier maximizes the ammonia content of the gas produced at the generator in order to obtain better performance for cooling production. In Configuration A (Figure 1), the rectification is effective for both the cooling and the power production lines, while in Configuration B the ammonia expended to produce power is not rectified as the switch valve directing the flow between the two production lines is positioned

before the rectifier. The two variations of the cycle exist in different architectures founded in the literature (Mendoza, Ayou, *et al.*, 2014; Kumar, Saravanan and Coronas, 2017).

To produce power, a superheater raises the temperature of the fluid to ensure that it remains in a gaseous state throughout the expansion. In the scroll expander, the fluid is then trapped and expanded in expansion chambers. By deforming, the chambers cause the rotation of a shaft that is coupled to a generator to produce electricity.

To produce cooling, a heat exchange with an intermediate temperature source (usually the ambient) condenses the ammonia flowing from the generator. A valve expands the ammonia to low temperature so it can take calories at the evaporator for cooling production. Finally, a subcooler allows the ammonia to be pre-cooled before it is expanded, by using the ammonia coming out of the evaporator.

The flows from the two production lines mix and are finally absorbed into the poor solution through cooling by a source of intermediate temperature (the same as the one used in the condenser).

3. Experimental devices

Two different devices provide data to setup the following numerical models: the scroll expander model is parametrized according to tests performed on an ORC test rig, and an absorption cycle is characterized to setup the other components in the model of the complete CCP cycle.

3.1 Organic Rankine Cycle

Scroll expanders ensure the continuous expansion of a fluid in closed chambers. This solution is therefore very relevant for small power applications with moderate flow rates (Dumont, Dickes and Lemort, 2017). A 1 kW Air Squared® scroll expander (model E15H022A-SH) was mounted on an existing ORC test rig (Landelle *et al.*, 2017). A preheater has also been added to the initial device to increase the range of test conditions. In detail, a Hydra-Cell pump ensures the circulation and pressure elevation of the fluid. A preheater and an evaporator transfer up to 18 kW of thermal energy to it. Then the gaseous fluid expands in the scroll expander by driving a generator. Finally, a series of three condensers, fed by the same cold source, liquefy the fluid before it returns to the pump.

As ammonia cannot be directly tested in the installation, another pure fluid serves to characterize the scroll expander. The choice is an HFC commonly used in the heat pump industry: R245fa. This refrigerant have already demonstrated its ability to produce energy by expansion in an expander (Declaye *et al.*, 2013; Giuffrida, 2014). Thanks to adaptation laws between fluids described by (Giuffrida, 2014), the characterization completed with R245fa allows to project the scroll behavior when operating with ammonia.

3.2 Absorption chiller

To characterize the other components in the studied CCP cycle, tests are performed on an existing water/ammonia absorption chiller device. This experimental cycle produces up to 5 kW of cold (at temperature from -10°C to 20°C) from a heat source at low-grade temperature (70°C to 130°C) and a source at intermediate temperature (15°C to 45°C). The operating pressures vary between 8 and 20 bar on the high pressure side and from 2 to 6 bar on the low pressure side. Details of the design of the device and its detailed description were the subject of a previous paper (Boudéhenn *et al.*, 2012). In short, the operation of the device is identical to that of the CCP cycle studied and presented above, without the electricity production line parallel to the cooling production. The tests carried out on the device make it possible to estimate the pinches of temperature, pressure drops and efficiencies associated with the various components also present in the CCP cycle.

4. Numerical Models

The two following models were implemented in the ‘Engineering Equation Solver’ (EES) environment to be solved. The calculated values of specified thermodynamic states come from EES’s database for pure ammonia and water/ammonia mixtures.

4.1 Expander scroll modelling

Lemort's semi-empirical model (Lemort *et al.*, 2009) has been used in many studies to explore the different operating conditions of a scroll expander (Giuffrida, 2014; Mendoza, Navarro-Esbrí, *et al.*, 2014). It quantitatively estimates the performance of an expander with a limited number of operating conditions (flow rates, pressures

and temperatures) at the inlet. In detail, the model decomposes the flow of fluid through the scroll into seven distinct thermodynamic transformations. It also takes into account the mechanical and thermal exchanges of the scroll with its environment. The equations specific to each transformation and balance are detailed in the reference publication (Lemort *et al.*, 2009).

Tab. 1: Scroll properties determined from experimental data with R245fa. The bold values identify the corrections for operation with ammonia.

	A_{in} (mm²)	$AU_{in,n}$ (W/K)	$AU_{out,n}$ (W/K)	AU_{amb} (W/K)	BVR	A_{leak} (mm²)	τ_{loss} (N.m)
R245fa	28	12	31,4	7,5	2,7	5,7	0,2
Ammonia	28	**6**	**14,7**	7,5	**1,9**	**1**	0,2

The design of the expander, the working fluids and the operating conditions are inputs of the model Tab.1 lists the parameters related to the nature of the expander. A_{in} is the flow cross-section of the fluid at the expansion inlet. $AU_{in,n}$, $AU_{out,n}$ and AU_{amb} are the heat exchange coefficients of a fictitious isothermal wall with, respectively, the fluid before expansion, the fluid after expansion and the ambient. The Built-in Volume Ratio (BVR) characterizes the volume expansion rate. A_{leak} represents the total leakage area related to the flow of fluid through the expander that does not produce work. Finally, τ_{loss} is a mechanical friction coefficient. All these parameters are determined by minimizing the differences between experimental measurements and model calculations. The scroll response (power generation, output temperature and flow rate) was experimentally measured through 30 tests performed on the previously introduced ORC test bench for different temperature and flow rate conditions over the operating range of the expander. The same tests were simulated with the model by imposing four input parameters: the scroll speed, the temperature of the inlet fluid and the pressures upstream and downstream of the expander. The difference between the numerical and experimental results is quantified by the error:

$$\varepsilon = \sum \left[\left(\frac{T_{out,exp} - T_{out,num}}{\overline{T_{out,exp}}} \right)^2 + \left(\frac{\dot{W}_{exp} - \dot{W}_{num}}{\overline{\dot{W}_{exp}}} \right)^2 + \left(\frac{\dot{m}_{exp} - \dot{m}_{num}}{\overline{\dot{m}_{exp}}} \right)^2 \right] \qquad \text{(eq. 1)}$$

T_{out}, $\dot{W}$ and $\dot{m}$ are respectively the expansion outlet temperature, the power output and the fluid mass flow rate. The *exp* and *num* indices distinguish experimental quantities from numerically calculated quantities. A genetic algorithm is used to minimize the error ε and determine the value of the parameters listed in Table 1. To assess the accuracy of the model, a comparison is made between the experimental measurements and the recalculated numerical values based on the newly determined parameters (Fig.2). It shows that the differences are less than 10% for 26 of the 30 configurations studied, what tends to validate the numerical approach.

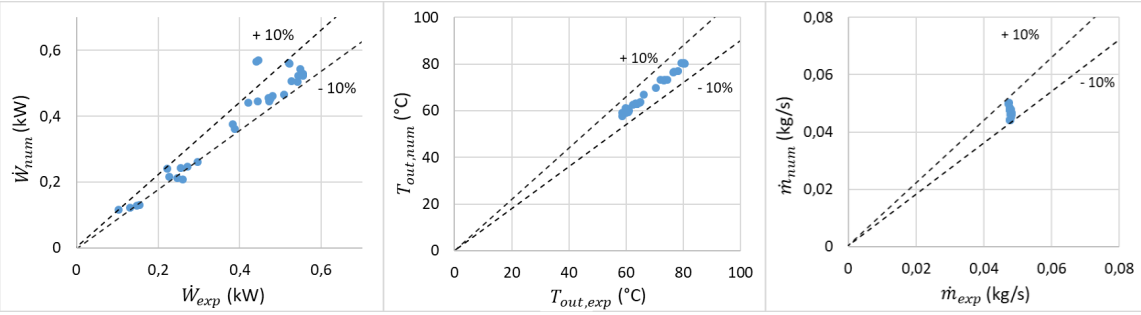

Fig.2 Comparison of numerical (vertical axis) and experimental (horizontal axis) results of $\dot{W}$, T_{out} and $\dot{m}$

The heat exchange coefficients of the model depend on both the properties of the scroll and the working fluid. In order to preserve the validity of a model calibrated on a type of scroll expander for different fluids, Giuffrida (2014) uses the intrinsic properties of the fluids to recalculate the heat exchange coefficients. Thus, the values of the exchange coefficients $AU_{in,n}$ and $AU_{out,n}$ determined for R245fa take the values of 6 W/K and 15.7 W/K respectively with ammonia. The study of an expander designed to operate with ammonia also requires adapting its geometry to be compatible with the properties of the fluid. Thus, since the expansion rate of ammonia is

significantly higher than that of R245fa, the BVR is reduced to 1.9 in the scroll expander model.

To evaluate the performance of the expander, its efficiency is defined as follows:

$$\eta_{expa} = \frac{\dot{W}}{\dot{m} . \Delta h_{is}} \qquad \text{(eq. 2)}$$

With Δh_{is} the enthalpy variation of the fluid in the scroll in the case of an isentropic transformation (ideal).

4.2 Influence of the position of the rectifier in the CFE cycle

A numerical model was developed based on the prototype of absorption cycle presented previously (Boudéhenn *et al.*, 2012). For each component, the energy and mass conservation equations were formalized. The experimentally set values of pinch, pressure drop and efficiency configure the heat exchanger model. Finally, it is assumed that the fluids are saturated at the outlet of each exchanger (except for an imposed superheating of 5 °C at the evaporator outlet). From this configuration, the model predicts the performance and thermodynamic states of the system for given operating conditions (temperature or power of the sources and solution mass flow rate).

To complete the development of the CCP cycle, the scroll expander model is integrated into the parallel absorption chiller model of the cold production circuit (see Figure 1). In addition, a superheater modelled as an adjustable power supply to the fluid precedes the scroll. In order to control the share of cold and electricity production, the split ratio r_s divides the refrigerant flow between the two production lines. It is equal to the ratio of the mass flow rate of ammonia passing through the evaporator to the mass flow rate of ammonia produced at the generator.

To estimate the cold production efficiency of the CCP cycle, the COP is defined as follows:

$$COP = \frac{Q_{evap}}{Q_{gen} . r_s} \qquad \text{(eq.3)}$$

With Q_{evap} the thermal power exchanged at the evaporator and Q_{gen} that at the generator.

In most of the following study, the split ratio r_s is set to 0.5, so distribution of generated ammonia is fair between the two production lines.

5. Results and analysis

A first analysis focuses on the operation of the scroll expander under the operating conditions of the CCP cycle and define a newly criteria to assess the quality of expanders. We then explore the performance of the complete cycle and carry out a comparative study between the two configurations of the cycle presented in Figure 1. Finally, a dual-objective optimization present the potential of cooling and power production of the cycle according to the temperatures of the sources.

5.1 Scroll performance under operating conditions of the CCP cycle

In a conventional absorption cycle, the flow of ammonia produced at the generator matches 20-30% of the flow of rich solution (Herold, Radermacher and Klein, 2016). Tests on the absorption chiller device estimate a maximum flow rate of fluid through the expander of about 0.01 kg/s. Fig.4 shows the power production of the scroll with ammonia as a function of flow rate. In order to highlight the sensitivity of the scroll performance to the low flow rate imposed by the CCP cycle (~ 0.01 kg/s), the study focuses on the influence of the following sensitive parameters: the pressure variation in the expander ΔP and the leakage area A_{leak}. We note that for a leakage area equivalent to that determined for the expander installed on the ORC test rig (solid curves), energy production is nil or very low for flows below 0.01 kg/s. Indeed, in this configuration, the internal leakages are too large compared to the ammonia flow and the scroll is not being driven. This effect is even more important as the pressure differential in the scroll is high (bold curves).

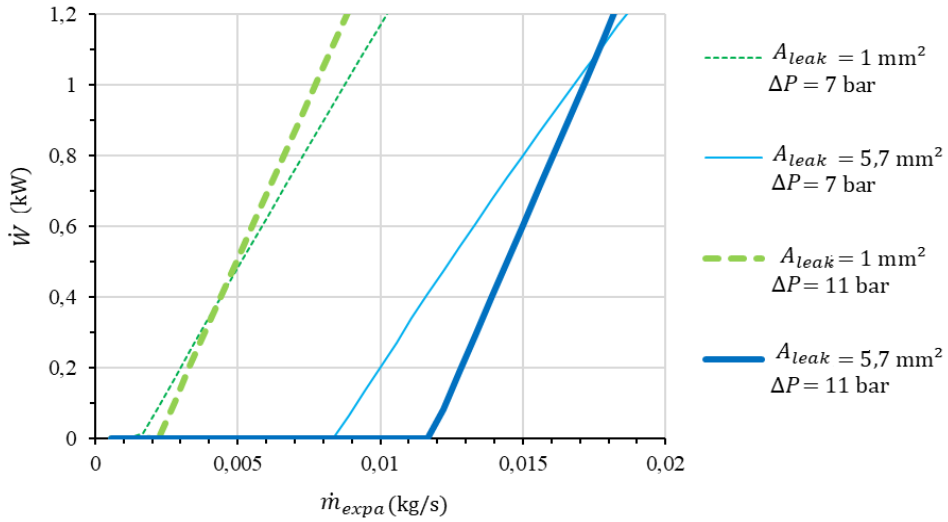

Fig. 3 Mechanical power produced by the scroll expander as a function of the leakage area and the pressure variation in the expander

With a leakage area reduced to 1 mm², the critical flow rate required to produce power is reduced to about 0.003 kg/s (dotted curves). As the leakage area is directly related to the volume efficiency of scroll expanders, this result illustrates the need to design highly efficient expanders for the development of small capacity CCP cycles. The reduced leakage area is retained for the rest of the study (A_{leak}= 1 mm²).

The characterization of leaks in expanders operating with ammonia is of major concerns as there are essential in the development of CCP cycle, Kalina cycle (Nag and Gupta, 1998) or ORC operating with ammonia. Considering a critical leakage area being the limit for A_{leak} above the one there is no power generation, it is relevant for expander constructors to evaluate this critical area easily from the foreseen operating conditions. The equations that governs the leaks in Lemort *et al.* (2009) publication involve numerous parameters. A sensitivity analysis stated that mostly the leakage area, the upstream pressure and the fluid nature influence the leakage mass flow rate. Considering ammonia as operating fluid, an evaluation of the leaks evolution, with variations of the two remaining parameters, enable to identify an analytical law to predict the critical mass flow rate:

$$A_{leak,c} = k\frac{\dot{m}_{expa}}{P_{in}} \qquad \text{(eq. 4)}$$

With k a constant consistent with speed unit and proper to the fluid. A regression of the mean square deviation between the law and the numerical prediction gives a value of k = 612.3 m/s for ammonia as working fluid. Finally, the prediction of the analytical law (eq. 4) fits with the numerical calculation of a critical leakage area with less than 3.7 % of relative error (see Fig. 4).

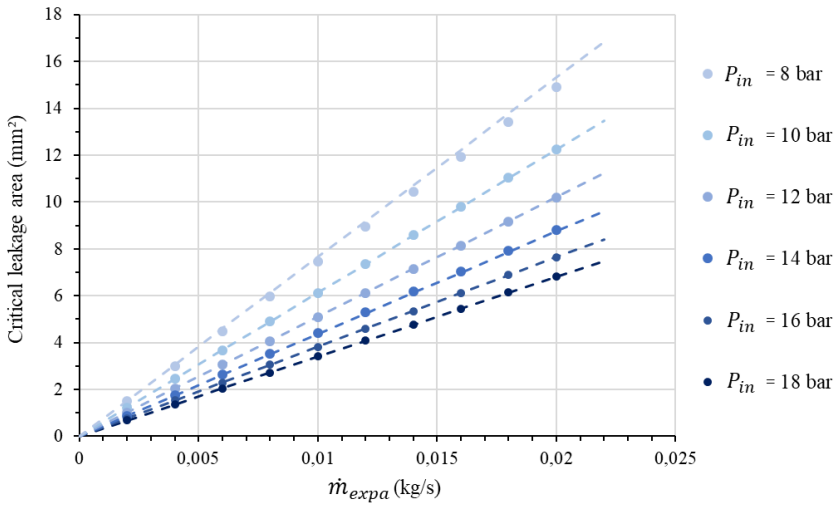

Fig.4 Numerical and analytical calculations of the critical leakage area of a scroll expander as a function of the ammonia mass flow rate and the pressure differential through the scroll.

The numerical data are computed for an inlet temperature of the fluid in the turbine of 110 °C and an outlet pressure of 4 bar. Nonetheless, sensitivity calculations show that the leakage mass flow rate varies less than 11 % for an input temperature between 90° and 160°C, with a slight leakage decrease when the temperature increases. Moreover, the outlet pressure doesn't act on the leakage numerical calculation unless it is greater than about 53 % of the inlet pressure, what is very rarely the case in ammonia absorption chiller. Thus, the scope of validity of the analytical law to estimate a critical leakage area (eq. 3) cover a large range of CCP cycles empoweredby low-grade temperature source (90°C to 160°C).

5.2 Impact of the rectification of ammonia for power production

To compare the two configurations of cycles previously introduced, this study analyses the action of the rectifier on the cycle performance. By lowering the temperature of the gas produced at the generator, the rectifier will condense the remaining traces of water in the ammonia and redirect them to the poor solution. Thus, the rectifier limits the water content in the ammonia, but also reduces the flow rate in the downstream production lines. To quantify the overall influence of the rectification on cycle efficiencies, Figure 5 shows, for both configurations, the expander efficiency (eq. 2) and the COP (eq. 3) of the cold production as a function of the mass fraction of ammonia in the evaporator. For the comparison, the cycle inputs are set as follow: the sources of hot, intermediate and cold temperatures are set respectively to 110°C, 27°C and 18°C; the rich solution flow rate is set at 0.028 kg/s; the superheater imposes an increase of temperature of 15°C between the generated ammonia and the inlet of the scroll.

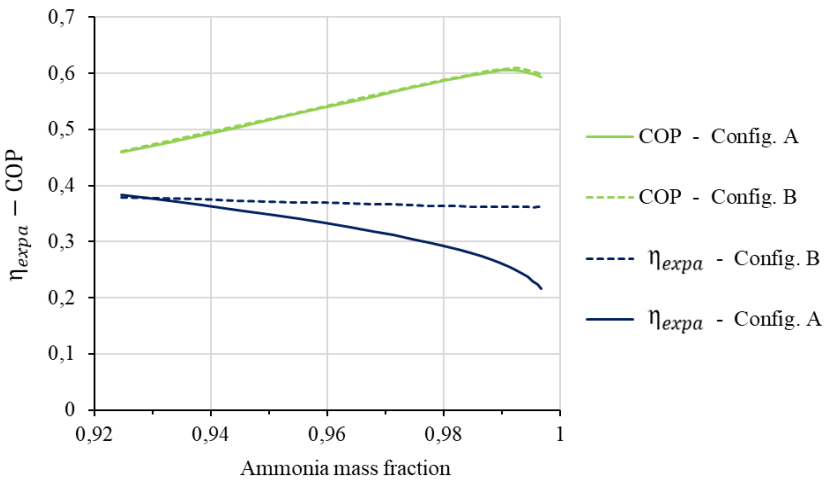

Fig.5 Expander efficiency and COP of the cooling production as a function of the mass fraction of ammonia at the evaporator.

The results confirm the relevance of the rectifier to improve the performance of cooling production as the COP increases to an optimum corresponding to an ammonia content of 99.2%. In addition, it can be observed that the COP is logically relatively unaffected by the cycle configuration since in both configurations the rectifier is always upstream of the cold production line.

Focusing on power production, the rectification of ammonia before it passes through the expander (configuration A) results in a significant decrease of the expander efficiency. For instance, an optimal rectification for cooling production (99.2% ammonia content) leads to a 34% reduction of the efficiency. This trend does not occur when the ammonia entering the expander is not rectified (configuration B). The decrease of the expander efficiency is then limited to 5% and is due to the reduction of the high pressure of the cycle, which is related to the rectification rate occurring on the cooling production line. Finally, this result makes it possible to establish that the loss of performance attributable to the presence of water vapor in the working fluid is less significant than that due to the reduction in flow rate caused by the rectification.

Note that other constraints (serial CCP cycle, combined generator-rectifier, etc.) may favor the choice of a less optimal configuration (type configuration A). Then the quantified comparison presented in this study can be used as a reference to arbitrate between different architectural options.

5.3 Dual optimization of the power and cooling production

A CCP cycle can produce power and cooling alternatively or simultaneously, but the optimal settings for each production mode are not all the same. In addition, the quantification of each production is not directly comparable as the cooling power is generally much higher than the mechanical/electrical power. Therefore, a tool that considers independently the power and the cooling production is necessary to perform a relevant optimization of the operational settings. Deb *et al.*, (2002) developed a multi-objective genetic algorithm. Coupled with the EES solver software, it is able to maximize both productions varying a defined number of optimizable parameters.

In this section, the most efficient configuration of the CCP cycle is considered (Configuration B). For the optimization algorithm, the three temperatures of the sources are the optimizable parameters and the only fixed input is the power exchanged at the generator that is set to 10 kW. The temperatures have the same boundaries than the absorption chiller test bench as described in a previous section. The pressures and the mass flow rates are all outputs of the modelling. The setting of the genetic algorithm is as follow: populations 1000 individuals, crossover probability of 0.9, mutation probability of 0.1 and 50 generations.

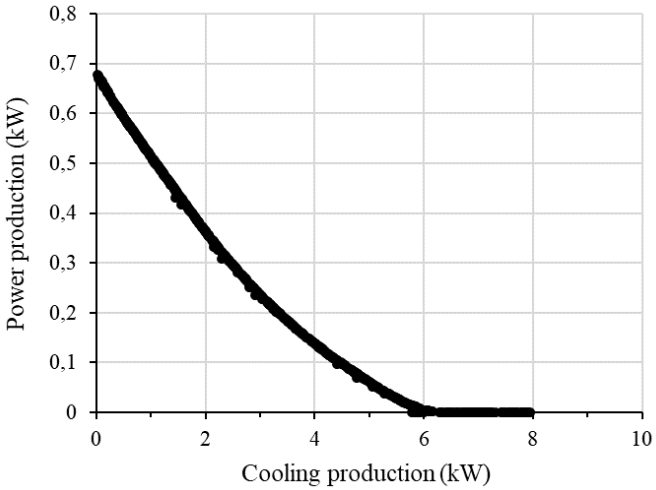

Fig. 6 Optimum frontier of the cooling and power productions obtained through a dual-optimization algorithm

The graph on Fig. 6 displays the optimum frontier obtained through the calculation of the dual-objective optimization. It firstly informs that functioning alternatively, the cycle can produce up to 680 W of power and 8 kW of cooling. Between these two extreme production modes, the plotted results show the maximum power and cooling production that can be produced simultaneously. One can notice that no power can be produce for cooling production greater than 6 kW. This effect is directly related to the mass flow rate passing through the expander. As cooling and power productions are set in parallel in the cycle, the flow rate through the expander decreases

with increasing cooling production and, as previously introduced, this one becomes too low to get over the leakage of fluid through the expander.

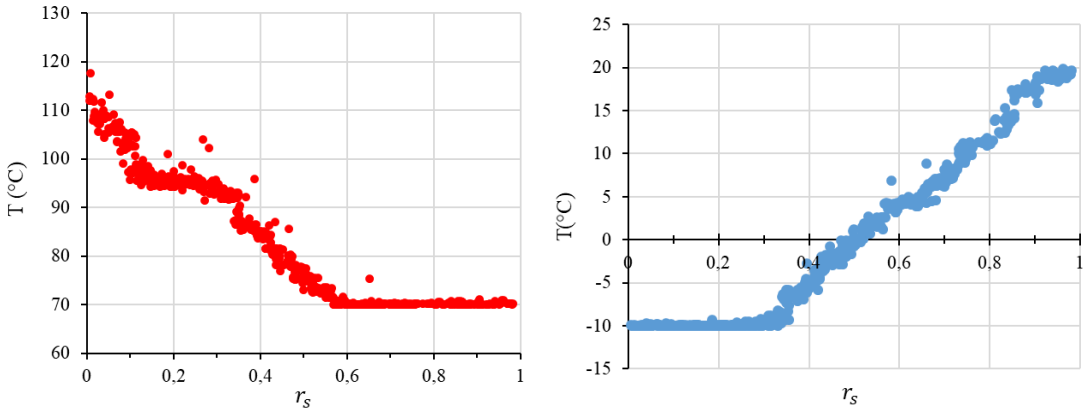

Fig.7 Evolution of the temperatures of the hot source (left) and of the cooling production (right) with the split ratio determined by to the dual-optimization algorithm

The graphs on Fig.7 display the evolution of both temperatures of hot source and cooling production from power production alone ($r_s = 0$) to cooling production alone ($r_s = 1$) and for all the in-between simultaneous production modes. It shows that the hot source temperature is preferentially higher for power production and lower for cooling production, while the opposite is observed for the cooling production temperature. The plateaus are a consequence of the imposed boundaries for the temperatures of the sources. Moreover, the temperature of the intermediate source of the CCP cycle (not displayed here), finds an optimum at its lowest boundary (15 °C) independently of the value of r_s. Those effects can easily be explained by the influence of the temperature on the operating pressures and mass flow rates and on the expansion potency of the ammonia that increases with the temperature. The results are also consistent with the preliminary experimental observations on both test benches.

6. Conclusion

Among the CCP cycle architectures under development, those in parallel are the most versatile and easiest to implement but they have not been widely investigated. To contribute to the development of these systems, a complete numerical model of the parallel CCP cycle was developed and configured through the characterization of two experimental devices: an ORC test rig to characterize a scroll expander and an absorption cycle to evaluate the rest of the system.

Early results highlighted the importance of using a detailed expander model to quantify the intrinsic physics of the flows in the scroll. Indeed, under the operating conditions of a small capacity machine, low flow rates require the use of high volume efficiency expanders. Moreover, an analysis focusing on the role and position of the rectifier in the cycle highlights its influence on the performance of power production. This result introduces a new criterion for cycle architecture optimization. Finally, a dual-objective optimization algorithm highlighted the potential of the CCP cycle and introduced some leanings to optimize the operating conditions according to the different production modes.

7. Acknowledgments

The French Alternative Energies and Atomic Energy Commission (CEA) and Carnot Energies du Futur supported this work.

8. References

Alexis, G. K. (2007) ‘Performance parameters for the design of a combined refrigeration and electrical power cogeneration system’, *International Journal of Refrigeration*, 30(6), pp. 1097–1103. doi: 10.1016/j.ijrefrig.2006.12.013.

Ayou, D. S. *et al.* (2013) ‘An overview of combined absorption power and cooling cycles’, *Renewable and*

Sustainable Energy Reviews. Elsevier, pp. 728–748. doi: 10.1016/j.rser.2012.12.068.

Boudéhenn, F. *et al.* (2012) 'Development of a 5 kW cooling capacity ammonia-water absorption chiller for solar cooling applications', *Energy Procedia*, 30, pp. 35–43. doi: 10.1016/j.egypro.2012.11.006.

Deb, K. *et al.* (2002) 'A fast and elitist multiobjective genetic algorithm: NSGA-II', *IEEE Transactions on Evolutionary Computation*, 6(2), pp. 182–197. doi: 10.1109/4235.996017.

Declaye, S. *et al.* (2013) 'Experimental study on an open-drive scroll expander integrated into an ORC (Organic Rankine Cycle) system with R245fa as working fluid', *Energy*. Elsevier Ltd, 55, pp. 173–183. doi: 10.1016/j.energy.2013.04.003.

Dumont, O., Dickes, R. and Lemort, V. (2017) 'Experimental investigation of four volumetric expanders', *Energy Procedia*. Elsevier B.V., 129, pp. 859–866. doi: 10.1016/j.egypro.2017.09.206.

Giuffrida, A. (2014) 'Modelling the performance of a scroll expander for small organic Rankine cycles when changing the working fluid', *Applied Thermal Engineering*. Elsevier Ltd, 70(1), pp. 1040–1049. doi: 10.1016/j.applthermaleng.2014.06.004.

Herold, K., Radermacher, R. and Klein, S. (2016) 'Absorption Chillers and Heat Pumps, Second Edition'. CRC Press. doi: 10.1201/b19625.

Khaliq, A. (2017) 'Energetic and exergetic performance investigation of a solar based integrated system for cogeneration of power and cooling', *Applied Thermal Engineering*. Elsevier Ltd, 112, pp. 1305–1316. doi: 10.1016/j.applthermaleng.2016.10.127.

Kumar, G. P., Saravanan, R. and Coronas, A. (2017) 'Experimental studies on combined cooling and power system driven by low-grade heat sources', *Energy*. Elsevier Ltd, 128, pp. 801–812. doi: 10.1016/j.energy.2017.04.066.

Landelle, A. *et al.* (2017) 'Performance investigation of reciprocating pump running with organic fluid for organic Rankine cycle', *Applied Thermal Engineering*. Elsevier Ltd, 113, pp. 962–969. doi: 10.1016/j.applthermaleng.2016.11.096.

Lemort, V. *et al.* (2009) 'Testing and modeling a scroll expander integrated into an Organic Rankine Cycle', *Applied Thermal Engineering*. Elsevier Ltd, 29(14–15), pp. 3094–3102. doi: 10.1016/j.applthermaleng.2009.04.013.

Mendoza, L. C., Navarro-Esbrí, J., *et al.* (2014) 'Characterization and modeling of a scroll expander with air and ammonia as working fluid', *Applied Thermal Engineering*, 70(1), pp. 630–640. doi: 10.1016/j.applthermaleng.2014.05.069.

Mendoza, L. C., Ayou, D. S., *et al.* (2014) 'Small capacity absorption systems for cooling and power with a scroll expander and ammonia based working fluids', *Applied Thermal Engineering*. Elsevier Ltd, 72(2), pp. 258–265. doi: 10.1016/j.applthermaleng.2014.06.019.

Muye, J. *et al.* (2016) 'Performance study of a solar absorption power-cooling system', *Applied Thermal Engineering*. Elsevier Ltd, 97, pp. 59–67. doi: 10.1016/j.applthermaleng.2015.09.034.

Nag, P. K. and Gupta, A. V. S. S. K. S. (1998) 'Exergy analysis of the kalina cycle', *Applied Thermal Engineering*, 18(6), pp. 427–439. doi: 10.1016/S1359-4311(97)00047-1.

Tauveron, N., Colasson, S. and Gruss, J. A. (2014) 'Available systems for the conversion of waste heat to electricity', in *Proceedings of the ASME 2014 International Mechanical Engineering Congress & Exposition*, pp. 1–12. doi: 10.1115/IMECE2014-37984.

Wang, J. *et al.* (2009) 'Parametric analysis for a new combined power and ejector-absorption refrigeration cycle', *Energy*. Elsevier Ltd, 34(10), pp. 1587–1593. doi: 10.1016/j.energy.2009.07.004.

Xu, F., Yogi Goswami, D. and S. Bhagwat, S. (2000) 'A combined power/cooling cycle', *Energy*, 25(3), pp. 233–246. doi: 10.1016/S0360-5442(99)00071-7.